Spatial–Temporal Equalization for IS-136 TDMA Systems with Rapid Dispersive Fading and Cochannel Interference

Ye (Geoffrey) Li, *Senior Member, IEEE,* Jack H. Winters, *Fellow, IEEE,* and Nelson R. Sollenberger, *Fellow, IEEE*

***Abstract*—In this paper, we investigate spatial–temporal equalization for IS-136 time-division multiple-access (TDMA) cellular/PCS systems to suppress intersymbol interference and cochannel interference and improve communication quality. This research emphasizes channels with large Doppler frequency (up to 184 Hz), delay dispersion under one symbol duration, and strong cochannel interference. We first present the structure of the optimum spatial–temporal decision-feedback equalizer (DFE) and linear equalizer and derive closed-form expressions for the equalizer parameters and mean-square error (MSE) for the case of known channel parameters. Since the channel can change within an IS-136 time slot, the spatial–temporal equalizer requires parameter tracking techniques. Therefore, we present three parameter tracking algorithms: the *diagonal loading minimum MSE algorithm*, which uses diagonal loading to improve tracking ability, the *two-stage tracking algorithm*, which uses diagonal loading in combination with a reduced complexity architecture, and the *simplified two-stage tracking algorithm*, which further reduces complexity to one $M \times M$ and one 3×3 matrix inversion for weight calculation with M antennas. For a four-antenna system, the simplified two-stage tracking algorithm can attain a 10^{-2} bit error rate (BER) when the channel delay spread is half of the symbol duration and the signal-to-interference ratio (SIR) of the system is as low as 5 dB, making it a computationally feasible technique to enhance system performance for IS-136 TDMA systems.**

***Index Terms*— Interference suppression, spatial–temporal equalization, time-varying channels.**

I. Introduction

ANTENNA arrays can be used in mobile wireless systems to mitigate rapid dispersive fading, suppress cochannel interference, and improve communication quality. For flat fading channels with antenna arrays, the *direct matrix inversion* (DMI) [1], [2] or the *diagonal loading DMI* (DMI/DL) [3] algorithm can be used to enhance desired signal reception and suppress interference effectively. In this paper, we study spatial–temporal equalization for dispersive fading channels with antenna arrays. Our investigation focuses on equalizer parameter tracking for IS-136 time-division multiple-access (TDMA) cellular/PCS mobile radio systems with rapid fading and strong cochannel interference.

For slow fading or time-invariant dispersive channels, where the channel parameters are available or easily estimated, decision-feedback equalization [4]–[6] and linear equalization are effective techniques to remove intersymbol interference and cochannel interference. System performance can be further improved if antenna arrays are combined with the equalizer. The structure and mean-square error (MSE) of the optimum diversity combiner and decision-feedback equalizer (DFE) or linear equalizer (LE) have been derived in [7]–[9] for channels with additive white Gaussian noise. For channels with both additive Gaussian noise and cochannel interference, many researchers [2], [10]–[12] have investigated the optimum diversity combiner and DFE or LE from different points of view. In particular, for systems with one antenna, Peterson and Falconer [11], [12] have studied the minimum MSE (MMSE) DFE and LE for strictly bandlimited channels. In this paper, we analyze the performance of the MMSE spatial–temporal DFE (MMSE-STDFE) and LE (MMSE-STLE) for antenna array systems with cochannel interference and derive closed-form expressions for the equalizer parameters and MMSE without this restriction.

Since the channel can change within an IS-136 time slot, the spatial–temporal equalizer (STE) requires adaptive algorithms to track the equalizer parameters. Blind channel equalization algorithms [13]–[17] have poor performance in IS-136 TDMA systems because of their slow convergence. Hence, training sequences are used to determine the initial setting of the STE and then the decided (or sliced) signals are employed to track the equalizer parameters. Even though for time-invariant channels with additive white Gaussian noise the maximum-likelihood sequence estimator (MLSE) is superior to the DFE and LE, the MLSE becomes extremely complicated for multiple-antenna systems with cochannel interference if spatial and temporal correlations for both the desired signal and interference are used. Hence, to reduce computational complexity, the MLSE in [18] and [19] uses temporal correlation for the desired signal only, which degrades its performance. On the other hand, with reasonable complexity, the STE uses spatial and temporal correlation for both the desired signal and interference and therefore may provide superior performance with lower complexity. Therefore, we investigate the STE for IS-136 TDMA systems.

This paper is organized as follows. Section II briefly describes our mathematical model of mobile radio systems with antenna arrays and some statistical properties for mobile wireless channels. Then, Section III derives closed-form expressions for the parameters and MSE of optimum spa-

Manuscript received February 12, 1997; revised May 28, 1997.

The authors are with the Wireless Systems Research Department, AT&T Labs-Research, Red Bank, NJ 07701-7033 USA.

Publisher Item Identifier S 0018-9545(99)05712-6.

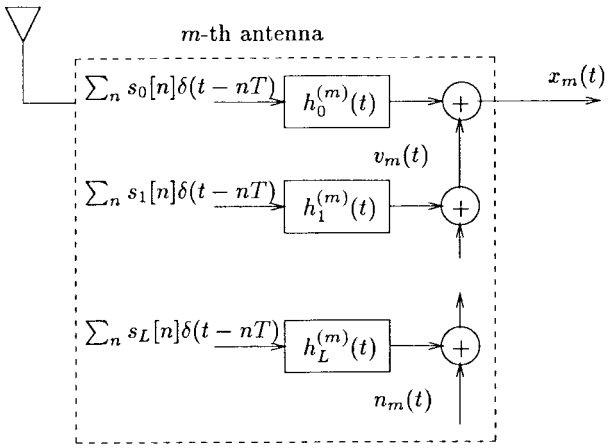

Fig. 1. System model.

tial–temporal equalization. Next, Section IV develops parameter tracking algorithms for the STE, including the *diagonal loading MMSE* (DLMMSE) and *two-stage tracking algorithms*. Finally, Section V presents computer simulation results of the performance of the STE in various environments.

II. System Model

For mobile wireless communication systems with M antennas, as shown in Fig. 1, the received signal at the mth sensor, $x_m(t)$, can be expressed in baseband form as

$$x_m(t) = \sum_{n=-\infty}^{\infty} h_0^{(m)}(t-nT)s_0[n] + v_m(t) \tag{1}$$

where $\{s_0[n]\}$ is the desired data from the transmitter, $h_0^{(m)}(t)$ is the combined channel and signal impulse response at the mth sensor corresponding to the desired data, and T is the symbol period. In IS-136 TDMA systems, the baud rate is $R_b = 24.3$ ksymbols/s and $T = 1/R_b$. $v_m(t)$ in (1) includes stationary and nonstationary interference, which can be written as

$$v_m(t) = \sum_{l=1}^{L} \sum_{n=-\infty}^{\infty} h_l^{(m)}(t-nT)s_l[n] + n_m(t). \tag{2}$$

In (2), $n_m(t)$ is the additive complex white Gaussian noise with two-sided power spectral density N_o, $s_l[n], l = 1, \cdots, L$ is the complex data of the lth interferer, and $h_l^{(m)}(t)$ is the combined impulse response of the mth sensor corresponding to the lth interferer. We will assume that both the transmitted and the interference data are *independent, identically distributed* (i.i.d.) complex zero-mean random variables with variance σ_s^2.

The received signals from the antenna arrays can be also expressed in vector form as

$$\boldsymbol{x}(t) = \sum_{l=0}^{L} \sum_{n=-\infty}^{\infty} \boldsymbol{h}_l(t-nT)s_l[n] + \boldsymbol{n}(t) \tag{3}$$

with

$$\boldsymbol{x}(t) \triangleq [x_1(t), \cdots, x_M(t)]^T \tag{4}$$

$$\boldsymbol{h}_l(t) \triangleq [h_l^{(1)}(t), \cdots, h_l^{(M)}(t)]^T \tag{5}$$

and

$$\boldsymbol{n}(t) \triangleq [n_1(t), \cdots, n_M(t)]^T. \tag{6}$$

In IS-136 TDMA systems, the shaping pulse is a square-root raised cosine with rolloff parameter $\beta = 0.35$, which is a real and symmetric function

$$c(t) = \int_{-\infty}^{\infty} C(f)e^{j2\pi ft}\, df \tag{7}$$

where

$$C(f) = \begin{cases} \sqrt{T} & 0 \le |f| \le (1-\beta)/2T \\ \sqrt{\dfrac{T}{2}\left[1 - \sin\left(\pi T \dfrac{f - 1/2T}{\beta}\right)\right]} & \\ & (1-\beta)/2T \le |f| \le (1+\beta)/2T \\ 0, & \text{otherwise.} \end{cases} \tag{8}$$

Therefore, the combined channel impulse response can be expressed as

$$h_l^{(m)}(t) = c(t) * g_l^{(m)}(t) \tag{9}$$

where * denotes convolution and $g_l^{(m)}(t)$ represents the multipath fading of wireless channel.

For a two-path Rayleigh fading channel model

$$g_l^{(m)}(t) = \alpha_{0,l}^{(m)}\delta(t) + \alpha_{1,l}^{(m)}\delta(t-t_d). \tag{10}$$

In the above expression, t_d is the delay spread between the two paths, which is usually less than T in IS-136 TDMA systems. We assume that $\alpha_{0,l}^{(m)}(t)$ and $\alpha_{1,l}^{(m)}(t), l = 1, \cdots, L$ and $m = 1, \cdots, M$ are narrow-band complex Gaussian processes, which are independent for different l's and m's. They have the same relative power spectral density [20]

$$\frac{p_\alpha(f)}{p_\alpha(0)} = \frac{1}{\sqrt{1-(f/f_d)^2}} \tag{11}$$

where f_d is the *Doppler frequency* which is related to the vehicle speed v and the carrier frequency f_c by

$$f_d = \frac{vf_c}{c} \tag{12}$$

where c is the speed of light. For systems with carrier frequency $f_c = 2$ GHz, the Doppler frequency can be as large as $f_d = 184$ Hz when the user is moving at 60 mi/h.

The two-path Rayleigh fading channel model is the standard channel model specified for IS-136 TDMA system and, furthermore, is considered as the worst case model. Hence, we have considered the two-path Rayleigh fading channel model for the results in this paper. However, the optimum STE presented in Section III and the parameter tracking approaches presented in Section IV do not rely on the specific channel model and, hence, are applicable to any channel.

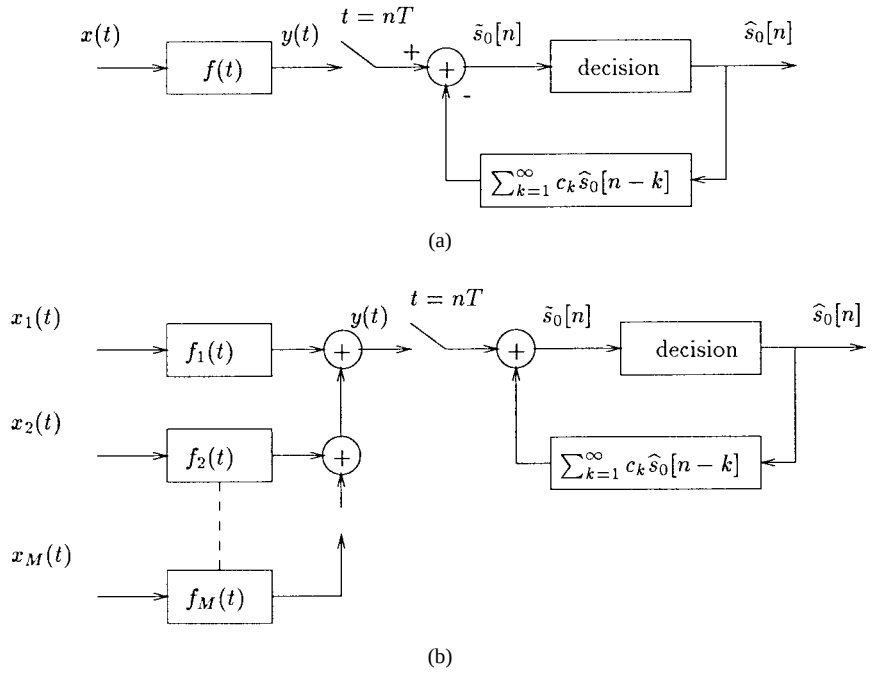

Fig. 2. MMSE-DFE for systems with cyclostationary interference.

III. Optimum Spatial–Temporal Equalizers

In this section, we study the *minimum MSE STE* (MMSE-STE) for channels with known statistical characteristics. We first introduce the MMSE-DFE and MMSE-LE for single-antenna systems with cyclostationary interference and then generalize the results to wireless systems with multiple antennas through a *single-channel equivalent model* [9]. We also investigate the general configuration of the MMSE-STE.

A. MMSE-DFE and MMSE-LE for Systems with Cyclostationary Interference

Petersen and Falconer [11], [12] have investigated the structures and MSE's of the MMSE-DFE and MMSE-LE in the frequency domain for strictly bandlimited channels. Below, we obtain closed-form expressions for the parameters and MSE's of the MMSE-DFE and MMSE-LE without this restriction. With bandlimited channels, our expressions appear different from, but are numerically equivalent to [11] and [12].

The MMSE-DFE for a one-antenna system with cyclostationary interference is shown in Fig. 2(a), which is similar to the MMSE-DFE for systems with stationary interference [6]. However, the expressions for $f(t)$ in the two cases are different although the derivation of the MMSE-DFE in both environments is similar. We highlight the difference in the derivations in the Appendix.

Define

$$r_{ij}(\omega) \triangleq \frac{1}{\tilde{N}_o T} \sum_{n=-\infty}^{\infty} H_i\Big(\frac{\omega}{2\pi} - \frac{n}{T}\Big) H_j^*\Big(\frac{\omega}{2\pi} - \frac{n}{T}\Big) \quad (13)$$

$$H_i(f) \triangleq \int_{-\infty}^{\infty} h_i(t) e^{-j2\pi ft}\, dt, \quad \tilde{N}_o \triangleq \frac{N_o}{\sigma_s^2} \quad (14)$$

and

$$\boldsymbol{R}(\omega) \triangleq [r_{ij}(\omega)]_{i,j=1}^{L} \quad \text{and} \quad \boldsymbol{r}(\omega) \triangleq [r_{10}(\omega), \cdots r_{L0}(\omega)]^T. \quad (15)$$

From the Appendix, the $f(t)$ for the MMSE-DFE in Fig. 2(a) is

$$f_o(t) = \frac{1}{\tilde{N}_0} \left\{ h_0^*(-t) - \sum_{k=-\infty}^{0} a_0[k] h_0^*(kT - t) - \sum_{l=1}^{L} \sum_{k=-\infty}^{\infty} a_l[k] h_l^*(kT - t) \right\} \quad (16)$$

and the MSE of the MMSE-DFE is

$$e\{f_o(t)\} = \sigma_s^2 \exp\left\{ -\frac{1}{2\pi} \int_{-\pi}^{\pi} \ln\{r(\omega) + 1\}\, d\omega \right\} \quad (17)$$

where

$$r(\omega) = r_{00}(\omega) - \boldsymbol{r}^H(\omega)[\boldsymbol{R}(\omega) + \boldsymbol{I}]^{-1} \boldsymbol{r}(\omega). \quad (18)$$

The parameter $a_l[n]$ in (16) can be calculated in frequency domain by

$$a_0(\omega) = 1 - \frac{1}{M(-\omega)\gamma_0} \quad a_0(\omega) \triangleq \sum_{n=-\infty}^{0} a_0[n] e^{-n\omega} \quad (19)$$

and

$$\boldsymbol{a}(\omega) = \frac{1}{M(-\omega)\gamma_0} [\boldsymbol{R}(\omega) + I]^{-1} \boldsymbol{r}(\omega) \quad (20)$$

$$a_l(\omega) \triangleq \sum_{n=-\infty}^{\infty} a_l[n] e^{j-n\omega}$$

$$\boldsymbol{a}(\omega) \triangleq [a_1(\omega), \cdots, a_L(\omega)]^T. \quad (21)$$

$M(\omega)$ in the above expression is a stable one-sided Fourier transform

$$M(\omega)=\sum_{n=0}^{\infty}\gamma_n e^{-jn\omega} \tag{22}$$

which is uniquely given by

$$M(\omega)M(-\omega)=r(\omega)+1. \tag{23}$$

γ_0 is given by

$$\gamma_0^2=\exp\left\{\frac{1}{2\pi}\int_{-\pi}^{\pi}\ln[r(\omega)+1]\,d\omega\right\}. \tag{24}$$

Following a similar derivation, the $f(t)$ and MSE for the MMSE-LE are

$$f_o(t)=\frac{1}{\tilde{N}_0}\left\{h_0^*(-t)-\sum_{l=0}^{L}\sum_{k=-\infty}^{\infty}a_l[k]h_l^*(kT-t)\right\} \tag{25}$$

and

$$e\{f_o(t)\}=\frac{\sigma_s^2}{2\pi}\int_{-\pi}^{\pi}\frac{1}{r(\omega)+1}\,d\omega. \tag{26}$$

The parameter $a_l[n]$ for the MMSE-LE is given by

$$\begin{aligned}a_0(\omega)&=\frac{r(\omega)}{1+r(\omega)}\\ \boldsymbol{a}(\omega)&=\frac{r(\omega)}{1+r(\omega)}\,[\boldsymbol{R}(\omega)+\boldsymbol{I}]^{-1}\boldsymbol{r}(\omega).\end{aligned} \tag{27}$$

where the definitions of $a_l(\omega)$, $l=1,\cdots,L$ and $\boldsymbol{a}(\omega)$ are the same as before, except that $a_0(\omega)$ is the two-sided Fourier transform defined as

$$a_0(\omega)\triangleq\sum_{n=-\infty}^{\infty}a_0[n]e^{-jn\omega}. \tag{28}$$

B. MMSE-STDFE and MMSE-STLE for Systems with Cyclostationary Interference

Using the *single-sensor equivalent model* developed in [9], we can easily extend the above results to multiple-antenna systems to derive the MMSE-STDFE and MMSE-STLE with cyclostationary interference.

For an M-antenna system, the *compounded channel impulse response* is defined as

$$\begin{aligned}h_l(t)=\sqrt{M}h_l^{(m)}\left(nT+M\left(t-nT-\frac{m-1}{M}T\right)\right)\\ nT+\frac{m-1}{M}T\le t<nT+\frac{m}{M}T\end{aligned} \tag{29}$$

and the *compounded channel additive noise* as

$$\begin{aligned}n(t)=\sqrt{M}n_m\left(nT+M\left(t-nT-\frac{m-1}{M}T\right)\right)\\ nT+\frac{m-1}{M}\,T\le t<nT+\frac{m}{M}T\end{aligned} \tag{30}$$

where $l=0,1,\cdots,L$, $m=1,\cdots,M$, and $n=0,\pm1,\pm2,\cdots$. According to [9], a single-antenna system with desired signal channel impulse response $h_0(t)$, interference channel impulse responses $h_i(t), i=1,\cdots,L$, and additive noise $n(t)$ is equivalent to the M-antenna system.

From the results established in the previous section, the $f(t)$ for the MMSE-DFE and MMSE-LE can be expressed as (16) and (25), respectively. Let

$$\boldsymbol{f}(t)\triangleq[f_1(t),\cdots,f_m(t)]^T. \tag{31}$$

Hence, by virtue of (29), the $\boldsymbol{f}(t)$ for the MMSE-STDFE in Fig. 2(b) is

$$\begin{aligned}\boldsymbol{f}_o(t)=\frac{1}{\tilde{N}_o}\Bigg\{\boldsymbol{h}_0^*(-t)-\sum_{k=-\infty}^{0}a_0[k]\boldsymbol{h}_0^*(kT-t)\\ -\sum_{l=1}^{L}\sum_{k=-\infty}^{\infty}a_l[k]\boldsymbol{h}_l^*(kT-t)\Bigg\}.\end{aligned} \tag{32}$$

The $\boldsymbol{f}(t)$ for the MMSE-STLE is

$$\boldsymbol{f}_o(t)=\frac{1}{\tilde{N}_o}\left\{\boldsymbol{h}_0^*(-t)-\sum_{l=0}^{L}\sum_{k=-\infty}^{\infty}a_l[k]\boldsymbol{h}_l^*(kT-t)\right\}. \tag{33}$$

The expressions of the parameter $a_i[n]$ and MSE for the MMSE-STDFE and MMSE-STLE are the same as those in the previous section except that $r_{ij}(\omega)$ is replaced by

$$\begin{aligned}r_{ij}(\omega)\triangleq\frac{1}{\tilde{N}_oT}\sum_{m=1}^{M}\sum_{n=-\infty}^{\infty}H_i^{(m)}\left(\frac{\omega}{2\pi}-\frac{n}{T}\right)\\ \cdot H_j^{(m)^*}\left(\frac{\omega}{2\pi}-\frac{n}{T}\right)\end{aligned} \tag{34}$$

where

$$H_i^{(m)}(f)=\int_{-\infty}^{\infty}h_i^{(m)}(t)e^{-j2\pi ft}\,dt. \tag{35}$$

Since $\boldsymbol{h}_l(t), l=0,1,\cdots,L$ usually differ, the concept of the *matched filter* for stationary interference systems is not valid here. Note that, if there is no cyclostationary interference, then the $\boldsymbol{f}_o(t)$ and the minimum MSE are the same as those in [7].

C. General Configuration of the MMSE-STE for Bandlimited Systems

For systems with only additive noise, the optimum MMSE-STE [7], [21] can be implemented using matched filters followed by a (discrete) T-spaced equalizer. Since the concept of a matched filter is not applicable for the systems with both additive noise and cochannel interference, a new structure has to be used. Hence, we investigate the configuration of the MMSE-STE for bandlimited systems with cochannel interference.

Let $s(t)$ be any $1/T$-bandlimited filter response whose spectrum satisfies

$$S(f)=\begin{cases}1, & |f|\le(1+\beta_o)/2T\\ 0, & |f|\ge 1/T\end{cases} \tag{36}$$

where β_o is the spectral flatness parameter. Note that $S(f)$, $(1+\beta_o)/2T<|f|<1/T$ can take any value that is square

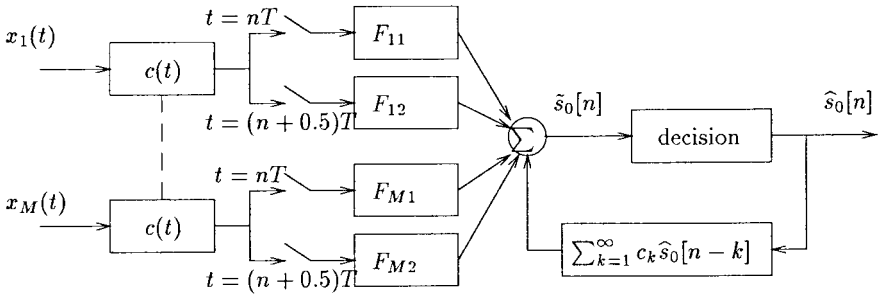

Fig. 3. General configuration of MMSE-STDFE for systems with cyclostationary interference.

integrable. Here, we set $\beta_o = \beta$, where β is the rolloff parameter of the shaping pulse (8), which is 0.35 in IS-136.

Since $s(t)$ is $1/T$ bandlimited, $c(t) * s(t) = c(t)$. Hence, for $l = 1, \cdots, L$ and $m = 1, \cdots, M$

$$\begin{aligned} h_l^{(m)}(t) &= c(t) * g_l^{(m)}(t) \\ &= c(t) * s(t) * g_l^{(m)}(t). \end{aligned} \tag{37}$$

Using the *sampling theorem,* we have

$$\begin{aligned} s(t) * g_l^{(m)}(t) &= \sum_{n=-\infty}^{\infty} g_l^{(m)}[n] s_o\left(t - n\frac{T}{2}\right) \\ &= s_o(t) * \left\{ \sum_{n=-\infty}^{\infty} g_l^{(m)}[n] \delta\left(t - n\frac{T}{2}\right) \right\} \end{aligned} \tag{38}$$

where

$$g_l^{(m)}[n] \triangleq \frac{T}{2} \int_{-\infty}^{\infty} s\left(n\frac{T}{2} - \tau\right) g_l^{(m)}(\tau)\, d\tau \tag{39}$$

$$s_o(t) \triangleq = \frac{2}{T} \frac{\sin(2\pi t/T)}{2\pi t/T}$$

$$S_o(f) = \mathcal{F}\{s_o(t)\} = \begin{cases} 1, & |f| \le 1/T \\ 0, & |f| > 1/T. \end{cases} \tag{40}$$

Hence

$$\begin{aligned} h_l^{(m)}(t) &= c(t) * s_o(t) * \left\{ \sum_{n=-\infty}^{\infty} g_l^{(m)}[n] \delta\left(t - n\frac{T}{2}\right) \right\} \\ &= c(t) * \left\{ \sum_{n=-\infty}^{\infty} g_l^{(m)}[n] \delta\left(t - n\frac{T}{2}\right) \right\} \\ &= c(t) * \left\{ \sum_{n=-\infty}^{\infty} g_l^{(m)}[2n] \delta(t - nT) \right\} + c\left(t - \frac{T}{2}\right) \\ &\quad * \left\{ \sum_{n=-\infty}^{\infty} g_l^{(m)}[2n+1] \delta(t - nT) \right\}. \end{aligned} \tag{41}$$

Substituting the above identity into (32), we have

$$\begin{aligned} f_o^{(m)}(t) &= c(t) * \left\{ \sum_{n=-\infty}^{\infty} f_{1,m}[n] \delta(t - nT) \right\} \\ &\quad + c\left(t - \frac{T}{2}\right) * \left\{ \sum_{n=-\infty}^{\infty} f_{2,m}[n] \delta(t - nT) \right\} \end{aligned} \tag{42}$$

where

$$\begin{aligned} f_{m,1}[n] = \frac{1}{\tilde{N}_o} \Bigg\{ & - g_l^{(m)*}[-2n] \\ & + \sum_{k=-\infty}^{0} a_0[k] g_0^{(m)*}[2k - 2n] \\ & + \sum_{l=1}^{L} \sum_{k=-\infty}^{\infty} a_l[k] g_l^{(m)*}[2k - 2n] \Bigg\} \end{aligned}$$

and

$$\begin{aligned} f_{m,2}[n] = \frac{1}{\tilde{N}_o} \Bigg\{ & - g_l^{(m)*}[-2n+1] \\ & + \sum_{k=-\infty}^{0} a_0[k] g_0^{(m)*}[2k - 2n + 1] \\ & + \sum_{l=1}^{L} \sum_{k=-\infty}^{\infty} a_l[k] g_l^{(m)*}[2k - 2n + 1] \Bigg\}. \end{aligned}$$

Hence, the MMSE-STDFE in Fig. 2(b) can be implemented as in Fig. 3, where $F_{m,i}$ for $m = 1, \cdots, M$ and $i = 1, 2$ are discrete filters with parameters $f_{m,i}[n]$. It can be shown that the MMSE-STLE has a similar structure to that in Fig. 3, but without the decision-feedback filter.

In IS-136 TDMA systems, $\beta = 0.35$. Hence, $s(t)$ in (36) can have many different values, which give multiple $g_l^{(m)}[n]$. Therefore, the parameter sets $f_{m,i}[n]$ for the MMSE-STE are not unique. For some pathological parameter sets, a small perturbation in the parameters can cause large performance degradation, and, therefore, the STE will not be robust in this case.

In the above discussion, we have assumed that the channels are time invariant. However, the derivation is also applicable to time-varying channels if the channel fade duration $(1/f_d)$ is much larger than the length of the channel impulse response, which is true in IS-136 TDMA systems.

IV. Parameter Tracking of Spatial–Temporal Equalizer

Once the channel parameters are known, the MMSE-STE can be implemented as in Fig. 3. As stated before, since the channel can change within an IS-136 time slot, the channel

parameters must be estimated. In this section, we investigate the parameter tracking of the STE.

A. MMSE-STE with Diagonal Loading

As shown in Fig. 3, in our MMSE-STDFE, a square-root raised-cosine *continuous* filter filters the received signal at each antenna, and then discrete filters enhance the signal and suppress interference. Practical communication systems use only finite length forward filters $F_{m,i}$ and feedback filter. The parameters of the forward and feedback filters are updated by decision-directed algorithms.

Let $\boldsymbol{u}[n]$ denote the *observation vector* at time $t = nT$, consisting of oversampled outputs from the square-root raised-cosine *continuous* filters and the previous decided symbols $\hat{s}_0[k]$ for $k < n$, and $\boldsymbol{w}[n]$ denote the *parameter vector* at time n consisting of the forward and feedback filter parameters.

The MMSE algorithm is a direct algorithm, which finds the $\boldsymbol{w}[n]$ that minimizes

$$C(\boldsymbol{w}[n]) = \frac{1}{N}\sum_{k=1}^{N} |\boldsymbol{w}^H[n]\boldsymbol{u}[n-k] - s_0[n-k]|^2\} \quad (43)$$

where N is the window length. In IS-136 TDMA systems, the training sequence contains 14 symbols. Hence, N is usually less than or equal to 14.

Direct calculation yields that the *parameter vector* $\boldsymbol{w}[n]$ that minimizes $C(\boldsymbol{w}[n])$ is

$$\boldsymbol{w}[n] = \boldsymbol{R}_u^{-1}[n]\boldsymbol{r}_{us}[n] \quad (44)$$

where

$$\boldsymbol{R}_u[n] \triangleq \frac{1}{N}\sum_{k=1}^{N} \boldsymbol{u}^H[n-k]\boldsymbol{u}[n-k]\} \quad (45)$$

and

$$\boldsymbol{r}_{su}[n] \triangleq \frac{1}{N}\sum_{1}^{N} \boldsymbol{u}[n-k]\}\hat{s}_0^*[n-k]. \quad (46)$$

In order for the STE to accurately track fast fading channels, the length of the window cannot be too long. Hence, the MMSE algorithm will have some estimation error. If it converges to a pathological parameter set, small parameter estimation error can cause large performance degradation. Therefore, the MMSE algorithm is not robust in all cases.

To keep the equalizer parameters from converging to pathological sets, we consider the use of diagonal loading, which finds the $\boldsymbol{w}[n]$ that minimizes the following cost function:

$$C(\boldsymbol{w}[n]) = \frac{1}{N}\sum_{k=1}^{N} |\boldsymbol{w}^H[n]\boldsymbol{u}[n-k] - s_0[n-k]|^2 + \gamma||\boldsymbol{w}[n]||^2 \quad (47)$$

where

$$\gamma = \sigma\ \mathrm{tr}\{\boldsymbol{R}_u[n]\}. \quad (48)$$

Here, $\mathrm{tr}\{\boldsymbol{R}_u[n]\}$ denotes the trace of $\boldsymbol{R}_u[n]$, which is the summation of the diagonal elements of $\boldsymbol{R}_u[n]$, and σ is the regularization factor. From (47), direct calculation yields

$$\boldsymbol{w}[n] = [\boldsymbol{R}_u[n] + \gamma\boldsymbol{I}]^{-1}\boldsymbol{r}_{us}[n]. \quad (49)$$

The regularization factor σ in (48) is a positive parameter that depends on the delay spread and the strength of the noise and interference, but good performance is typically achieved for σ between 0.001 and 0.01. The above algorithm is called the *diagonal loading MMSE (DLMMSE) algorithm*, which is one form of DMI/DL for spatial processing in [3]. Note that if the interference-to-noise ratio is known *a priori* or can be determined, better performance can generally be obtained with γ determined by [3, eq. (31)], rather than (48).

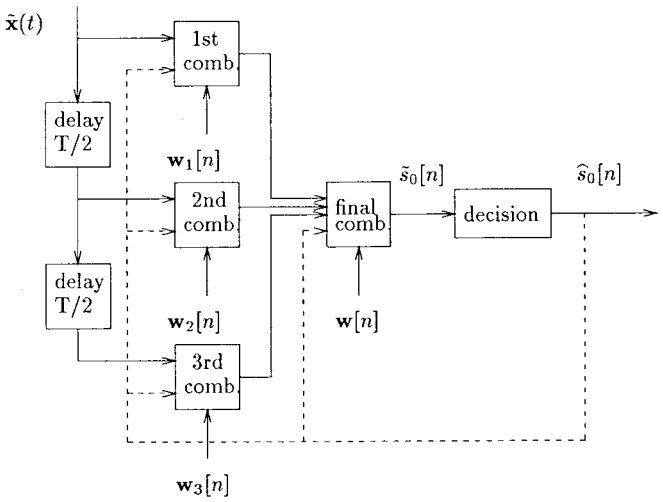

Fig. 4. Two-stage STE for systems with cyclostationary interference.

B. Two-Stage Tracking Algorithms

The DLMMSE algorithm requires inversion of a matrix which has a length given by the total number of spatial–temporal parameters and therefore can be computationally intensive. For example, if the forward filter at each antenna has two taps and the feedback filter has one tap in Fig. 3, then for four-antenna systems, a 9×9 matrix inversion is required to compute the filter parameters, which can be difficult for real-time implementation.

In [22], a space–time decomposition algorithm has been proposed for the STE to reduce the computational complexity when interference is not present. With interference, we propose a modified version of the STE of [22] as shown in Fig. 4, and combine it with the DLMMSE algorithm.

In this STE, $\tilde{\boldsymbol{x}}(nT - T/2)$, $\tilde{\boldsymbol{x}}(nT)$, and $\tilde{\boldsymbol{x}}(nT + T/2)$ are combined at the first, second, and third combiners, respectively. The weighting vector $\boldsymbol{w}_i[n]$ is estimated for each combiner by the DLMMSE algorithm using $\tilde{\boldsymbol{x}}(nT + (i-2)T/2)$ as the observation vector and $\hat{s}_0[n]$ as the reference signal. That is, $\boldsymbol{w}_i[n]$ is calculated by

$$\boldsymbol{w}_i[n] = (\boldsymbol{R}_i[n] + \gamma\boldsymbol{I})^{-1}(\boldsymbol{r}_i[n] \quad (50)$$

where

$$\boldsymbol{R}_i[n] = \frac{1}{N}\sum_{k=1}^{N} \tilde{\boldsymbol{x}}(nT - kT + (i-2)T/2)$$

$$\cdot \tilde{\boldsymbol{x}}^H(nT - kT + (i-2)T/2) \tag{51}$$

$$\boldsymbol{r}_i[n] = \frac{1}{N}\sum_{k=1}^{N} \tilde{\boldsymbol{x}}(nT - kT + (i-2)T/2)\hat{s}_0^*[n-k]. \tag{52}$$

Hence, the output of the first stage combiner is

$$y_i[n] = \boldsymbol{w}_i^H[n]\tilde{\boldsymbol{x}}(nT + (i-2)T/2). \tag{53}$$

The weighting vector $\boldsymbol{w}[n]$ at the final combiner is calculated by

$$\boldsymbol{w}[n] = (\boldsymbol{R}[n] + \gamma \boldsymbol{I})^{-1}\boldsymbol{r}[n] \tag{54}$$

where

$$\boldsymbol{R}[n] = \begin{pmatrix} R_{11}[n] & R_{12}[n] & R_{13}[n] \\ R_{21}[n] & R_{22}[n] & R_{23}[n] \\ R_{31}[n] & R_{32}[n] & R_{33}[n] \end{pmatrix} \tag{55}$$

$$R_{ij}[n] \triangleq \frac{1}{N}\sum_{k=1}^{N} \boldsymbol{w}_i^H[n]\tilde{\boldsymbol{x}}[nT - kT - (i-2)T/2] \cdot \tilde{\boldsymbol{x}}^H[nT - kT - (j-2)T/2]\boldsymbol{w}_j[n]) \tag{56}$$

and

$$\boldsymbol{r}[n] = (r_1[n], r_2[n], r_3[n])^T \tag{57}$$

$$r_i \triangleq \frac{1}{N}\sum_{k=1}^{N} \boldsymbol{w}_i^H[n]\tilde{\boldsymbol{x}}[nT - kT + (i-2)T/2]\hat{s}_0^*[n-k]. \tag{58}$$

Hence, the output signal is given by

$$\tilde{s}_0[n] = \boldsymbol{w}^H[n]\begin{pmatrix} y_1[n] \\ y_2[n] \\ y_3[n] \end{pmatrix}. \tag{59}$$

We call the equalizer that uses the above *two-stage tracking algorithm* a *two-stage STLE*. Decision-feedback can be used at either the first stage combiners or the second stage combiner. Hence, we refer to these equalizers as the *first-stage STDFE* and the *second-stage STDFE*, respectively.

For an M-antenna system, a two-stage STLE requires two $M \times M$ and one 3×3 matrix inversion, since $\boldsymbol{R}_1[n] = \boldsymbol{R}_3[n-1]$. However, the computation in the two-stage STLE can be further reduced if we calculate $\boldsymbol{w}_2[n]$ by

$$\boldsymbol{w}_2[n] = \tfrac{1}{2}\left[(\boldsymbol{R}_3[n] + \gamma \boldsymbol{I})^{-1} + (\boldsymbol{R}_3[n-1] + \gamma \boldsymbol{I})^{-1}\right]\boldsymbol{r}_2[n] \tag{60}$$

which eliminates the calculation of $\boldsymbol{R}_2[n]$. We call this equalizer a *simplified two-stage STLE*, since it requires only one $M \times M$ and one 3×3 matrix inversion.

V. Performance Evaluation Through Computer Simulations

The performance of the STE has been evaluated through computer simulation, which focused on its application in IS-136 TDMA systems. The simulation uses the system model described in Section II. Each time slot contains a 14-symbol training sequence followed by 134 symbols randomly drawn from $\{(1 + j/\sqrt{2}), (1 - j\sqrt{2}), (-1 + j/\sqrt{2}), (-1 - j/\sqrt{2})\}$. The parameters of the equalizers are initially estimated using the training sequence, and after the training period, they are tracked using decided (sliced) symbols. DQPSK modulation is used with coherent detection. The four-antenna system has white Gaussian noise and a single cochannel interferer, whose powers are given by the signal-to-noise ratio (SNR) and the signal-to-interference ratio (SIR), respectively. The channels use the two-path model with the same average power for each path, the same delay spread for both desired and interference channels, and $f_d = 184$ Hz, unless otherwise specified. The signal received by each antenna is first passed through a square-root raised-cosine filter and then oversampled at the ideal sampling time at a rate of $2/T$ for the STE. The desired signal and interference are time aligned for the results presented in this section (note that the relative timing does not significantly affect the performance of the STE). One feedback tap is used for the STDFE. To give insight into the average behavior of the STE in various environments, we have averaged the performance over 1000 time slots.

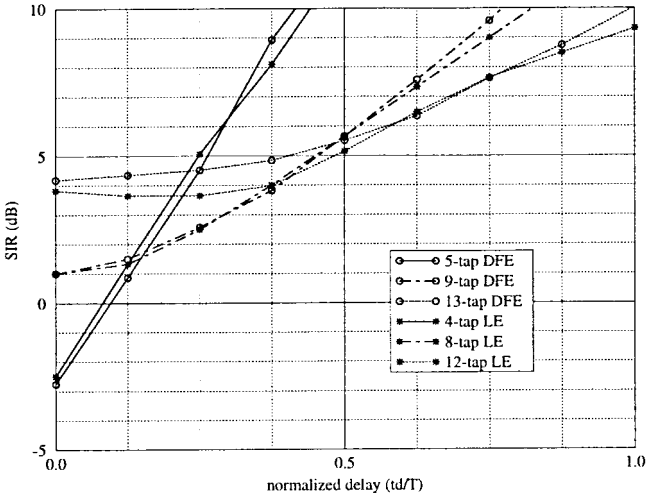

Fig. 5. Performance of DLMMSE-STDFE and DLMMSE-STLE: required SIR for BER $= 10^{-2}$ versus t_d with $f_d = 184$ Hz and SNR $= 20$ dB.

Fig. 5 shows the required SIR for a bit error rate (BER) $= 10^{-2}$ of different length DLMMSE-STE's for channels with SNR $= 20$ dB and different t_d's. From the figure, without delay spread, both the five-tap DLMMSE-DFE and four-tap DLMMSE-LE, i.e., spatial processing only, operate up to -2.5-dB SIR. With increasing t_d, the equalizer's interference suppression ability is reduced. As t_d increases, the equalizer performance is generally improved by increasing the number of taps. However, for rapid dispersive fading channels, a too-long equalizer does not necessarily have good performance because the parameter tracking performance degrades with increasing equalizer length, even through the longer equalizer always performs better than the shorter one with the optimum equalizer parameters. Hence, in Fig. 5, the five-tap DLMMSE-DFE and four-tap DLMMSE-LE have the best performance if $t_d \leq T/8$, while the 13-tap DLMMSE-STDFE and 12-tap DLMMSE-STLE have the best performance if $t_d > T/2$. Usually $t_d < T/2$ in IS-136 TDMA systems [24], therefore, the nine-tap DLMMSE-STDFE and eight-tap DLMMSE-STLE are two of the best STE's.

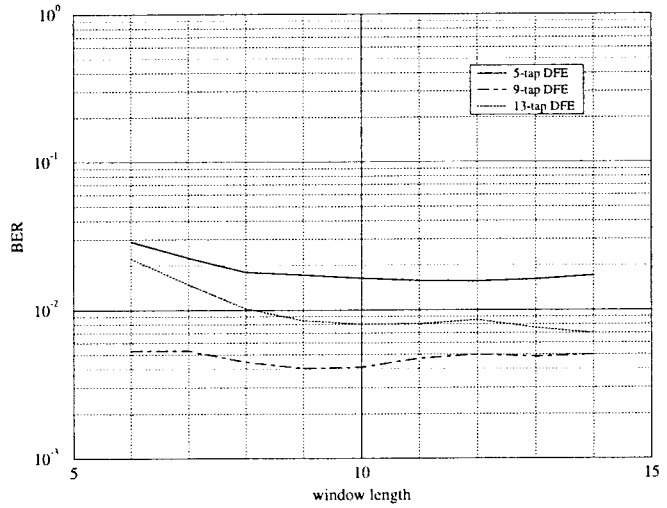

Fig. 6. BER versus window length for DLMMSE-DFE with $f_d = 184$ Hz, SNR $= 20$ dB, SIR $= 5$ dB, and $t_d = 1/4T$.

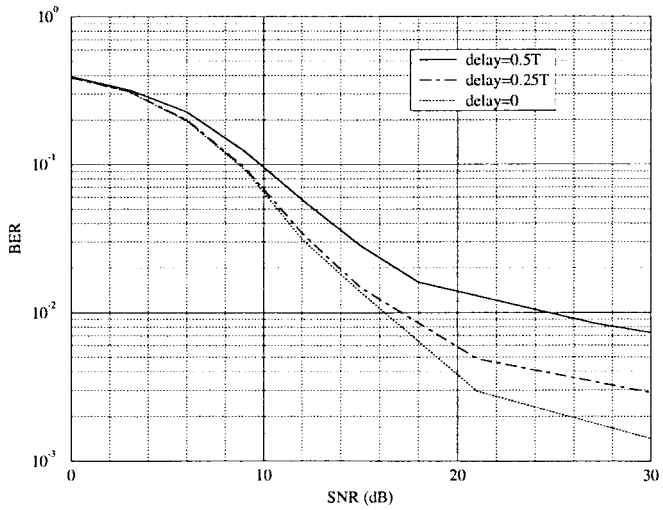

Fig. 8. Effect of SNR on BER of nine-tap DLMMSE-STDFE with $f_d = 184$ Hz, SIR $= 5$ dB, and different t_d's.

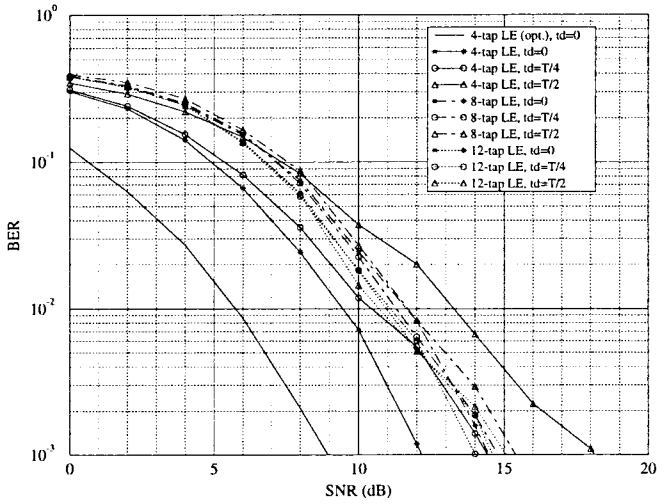

Fig. 7. Effect of SNR on BER of different length DLMMSE-STLE's with $f_d = 184$ Hz, SIR $= +\infty$, and different t_d's.

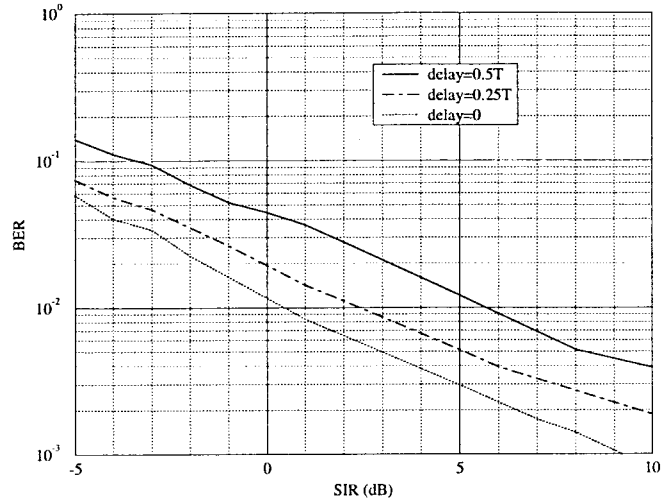

Fig. 9. Effect of SIR on BER of nine-tap DLMMSE-STDFE with $f_d = 184$ Hz, SNR $= 20$ dB, and different t_d's.

The performance of the DLMMSE-STE is not sensitive to the length of the window used to estimate the equalizer's parameters, as shown by Fig. 6.

Fig. 7 shows the BER versus SNR for channels with different t_d's and without cochannel interference when the DLMMSE STLE uses the optimum σ for interference suppression. Without delay spread, the four-tap equalizer attains a 10^{-2} BER when the SNR is 9.5 dB. However, if $t_d = T/2$, the SNR must be greater than 14 dB to maintain the same BER. However, for both the eight-tap STLE and the 12-tap STLE, the required SNR for a given BER varies by only about 1 dB for all channels with $t_d < T/2$.

If we know that the system has no intersymbol and cochannel interference, we can select σ to optimize the performance. For example, a four-tap spatial equalizer with the optimum σ for channels without delay spread will attain a 10^{-2} BER at SNR $= 6$ dB, which is about 3.5 dB better than that of the equalizer with the optimum σ for interference suppression.

Figs. 8 and 9 show the BER of a nine-tap DLMMSE-DFE for different SNR's, SIR's, and t_d's. In particular, for channels with $t_d = 0.25T$, the nine-tap STDFE attains a 10^{-2} BER when SIR $= 5$ dB, SNR $= 17$ dB or SIR $= 2.5$ dB, SNR $= 20$ dB.

Figs. 10 and 11 show the required SIR of a nine-tap STDFE for BER $= 10^{-2}$ when the two-path fading channel has different f_d's or unequal average power ratios r's. From Fig. 10, with decreasing f_d, the required SIR is reduced dramatically. For channels with $f_d = 184$ Hz and $t_d = T/2$, the required SIR for a 10^{-2} BER is 6 dB, while it is as low as -10 dB with $f_d = 10$ Hz. According to Fig. 11, the STE has the worst performance with the two-path fading channel with equal average power. Hence, we have selected the equal average power two-path fading channel model for most of our simulations.

Fig. 12 shows the performance of a two-stage STLE. Compared with the 5-tap, 9-tap, or 13-tap DLMMSE-STDFE, the

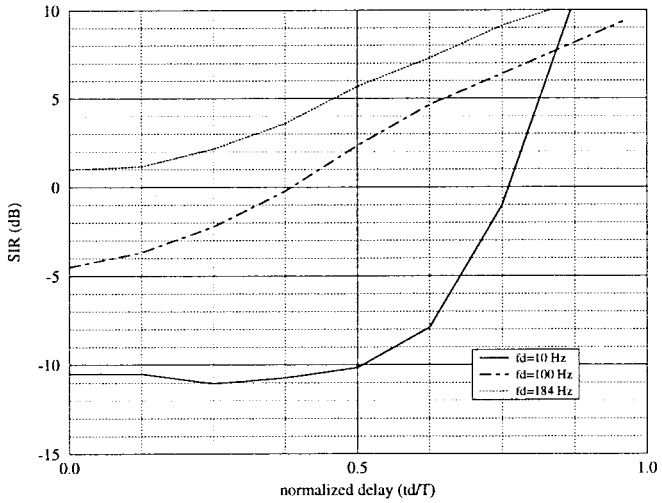

Fig. 10. Effect of t_d on required SIR of nine-tap DLMMSE-STDFE for BER $= 10^{-2}$ with SNR $= 20$ dB and different f_d's.

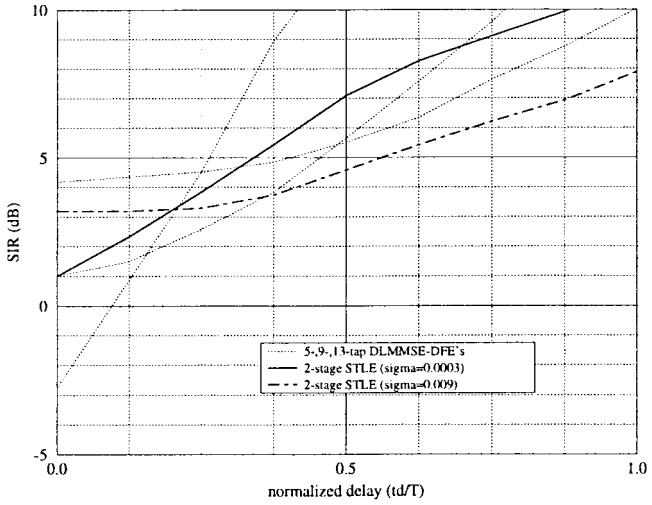

Fig. 12. Effect of t_d on required SIR of two-stage STLE for BER $= 10^{-2}$ with $f_d = 184$ Hz and SNR $= 20$ dB.

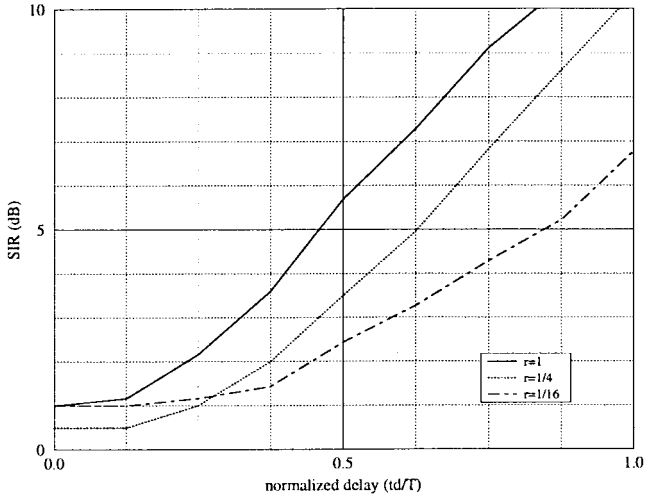

Fig. 11. Effect of t_d on required SIR of nine-tap DLMMSE-STDFE for BER $= 10^{-2}$ for unequal average power two-path channels with different average power ratios, $f_d = 184$ Hz, and SNR $= 20$ dB.

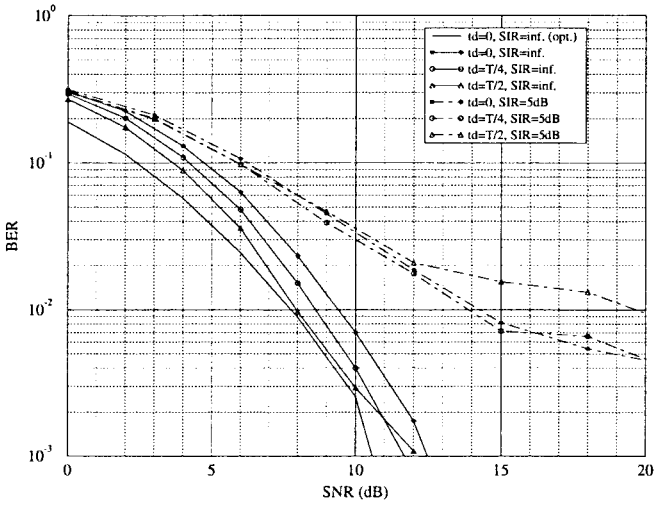

Fig. 13. Effect of SNR on BER of two-stage STLE ($\sigma = 0.009$) with $f_d = 184$ Hz, different t_d's, and SIR's.

two-stage equalizer has less sensitive required SIR curves. Considering the computation complexity and noise and interference suppressing performance, the two-stage STLE is preferred over the DLMMSE-STDFE.

Figs. 13 and 14 show the BER of the two-stage STLE under various conditions. Compared with Figs. 8 and 9, the two-stage STLE has stronger noise suppressing ability, but weaker interference suppressing ability than the nine-tap STDFE.

Figs. 15 and 16 show the required SIR of the two-stage STLE for two-path channel with different t_d's or unequal average powers for each path. Similar to the nine-tap DLMMSE-DFE, as the average power ratio r between two paths decreases, the curves become flatter. The required SIR decreases with decreasing t_d.

Fig. 17 compares the required SIR for a 10^{-2} BER for the original and simplified two-stage STLE. Compared with the original two-stage STLE, the simplified STLE has only about a 0.5-dB degradation when $t_d \leq 0.5T$. However, it has almost the same performance when $t_d > 0.5T$.

VI. Conclusions

In this paper, we have investigated spatial–temporal equalization for IS-136 TDMA systems to mitigate intersymbol interference and suppress cochannel interference, and thereby enhance system performance. With known channel parameters, we have derived the structure and the MSE of the MMSE-STE for multiple-antenna systems with cochannel interference. The MMSE-STE can be implemented as a continuous pulse shaping filter followed by fractionally spaced discrete filters at each antenna. However, the optimum parameter sets are not unique. For some pathological parameter sets, small perturbations on the parameters can cause large performance degradation, which explains why the MMSE parameter tracking algorithm is not robust in some cases. Hence, we developed the *diagonal loading MMSE-STE* and the *two-stage tracking STE* to keep the STE from converging to the pathological parameter sets. Furthermore, to reduce the computational complexity, we developed a *simplified two-stage tracking STLE*, which

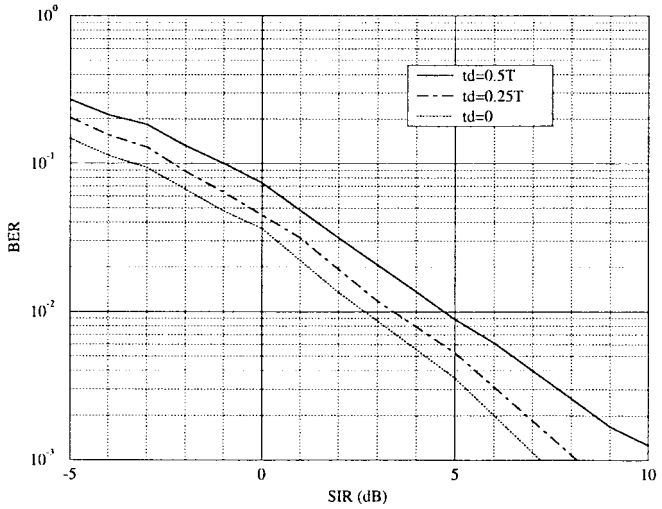

Fig. 14. Effect of SIR on BER of two-stage STLE ($\sigma = 0.009$) with $f_d = 184$ Hz, SNR $= 20$ dB, and different t_d's.

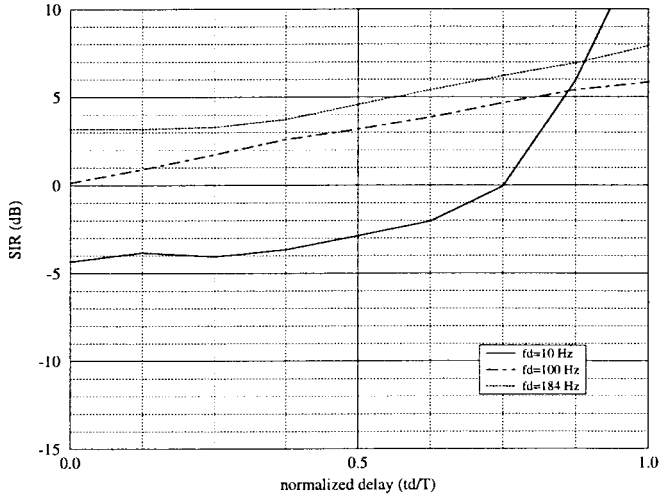

Fig. 15. Effect of t_d on required SIR of two-stage STLE for BER $= 10^{-2}$ with SNR $= 20$ dB and different f_d's.

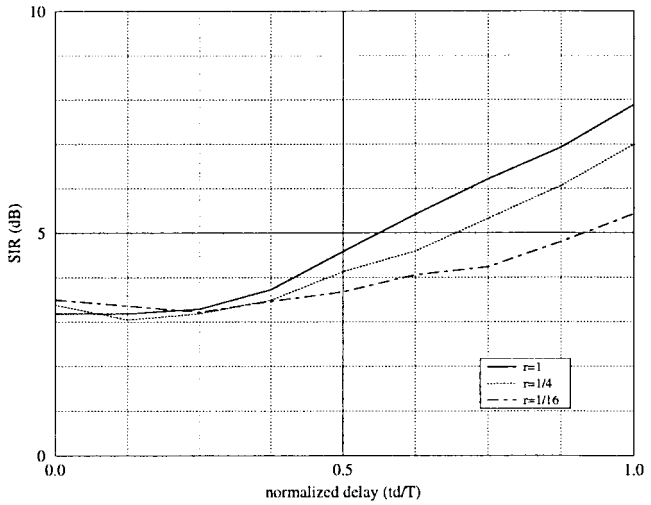

Fig. 16. Effect of t_d on required SIR of two-stage STLE for BER $= 10^{-2}$ for an unequal average two-path channel with different power ratios r, $f_d = 184$ Hz, and SNR $= 20$ dB.

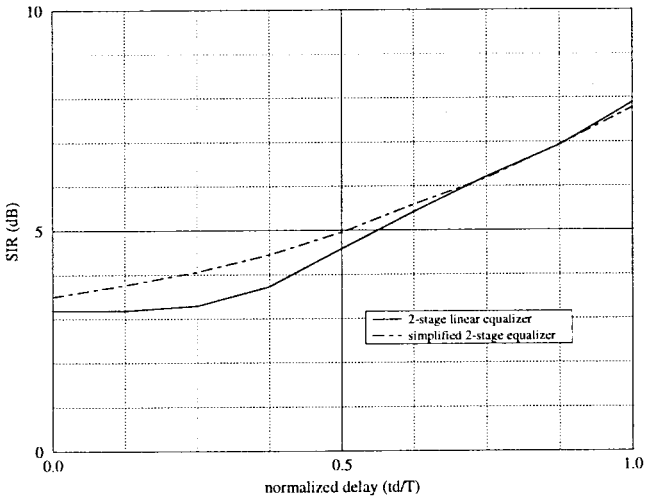

Fig. 17. Comparison of required SIR for the original and simplified two-stage STLE with $f_d = 184$ Hz and SNR $= 20$ dB.

requires only one $M \times M$ and one 3×3 matrix inversion for M-antenna systems, but can attain a 10^{-2} BER for $t_d = T/2$, $f_d = 184$ Hz, and SIR $= 5$ dB. Hence, considering performance and complexity, the simplified two-stage STLE is a promising technique for IS-136 TDMA systems.

APPENDIX
COEFFICIENT DERIVATION OF THE OPTIMUM DFE

Let the receiving filter $f(t)$ in Fig. 2(a) have square-integrable impulse response $f(t)$. Then the output of the receiving filter is

$$y(t) \triangleq \int f(\tau)x(t-\tau)\,d\tau. \tag{A-1}$$

The output of the equalizer is

$$\tilde{s}[n] \triangleq y(nT) - \sum_{k=1}^{\infty} c_k \hat{s}_0[n-k]$$

$$= \sum_{l=0}^{L} \sum_{k=-\infty}^{\infty} \int f(\tau)h_l(kT-\tau)\,d\tau s_l[n-k] + \int f(\tau)w(nT-\tau)\,d\tau - \sum_{k=1}^{\infty} c_k \hat{s}_0[n-k]. \tag{A-2}$$

If the decided symbols are all correct, the intersymbol interference caused by $s_0[k]$ for $k < n$ can be eliminated by selecting

$$c_k = \int f(\tau)h_0(kT-\tau)\,d\tau. \tag{A-3}$$

If the data $s_l[n]$ are i.i.d. random variables, the MSE of the equalizer output is

$$e\{f(t)\} \triangleq E\{|\tilde{s}[n] - s_0[n]|^2\} = \sigma^2 \left| \int f(\tau)h_0(-\tau)\,d\tau - 1 \right|^2$$

$$+\sigma^2\sum_{k=-\infty}^{-1}\left|\int f(\tau)h_0(kT-\tau)\,d\tau\right|^2 +\sigma^2\sum_{l=1}^{L}\sum_{k=-\infty}^{\infty}\left|\int f(\tau)h_l(kT-\tau)\,d\tau\right|^2 +N_o\int|f(\tau)|^2. \tag{A-4}$$

Using calculus of variations, we can show that the $f(t)$ that minimizes the MSE satisfies

$$f_o(t)=-\frac{1}{\tilde{N}_o}\left\{(a_0[0]-1)h_0^*(-t)+\sum_{k=-\infty}^{-1}a_0[k]h_0^*(kT-t)+\sum_{l=1}^{L}\sum_{k=-\infty}^{\infty}a_l[k]h_l^*(kT-t)\right\} \tag{A-5}$$

where

$$a_l[k]\triangleq\int f_o(\tau)h_l(kT-\tau)\,d\tau \tag{A-6}$$

and

$$\tilde{N}_o=\frac{N_o}{\sigma_s^2}. \tag{A-7}$$

Multiplying both sides of (A-5) by $h_l(nT-\tau)$ and using (A-6), we have

$$a_i[n]=-\left\{(a_0[0]-1)r_{i0}[n]+\sum_{k=-\infty}^{-1}a_0[k]r_{i0}[n-k]+\sum_{j=1}^{L}\sum_{k=-\infty}^{\infty}a_j[k]r_{ij}[n-k]\right\} \tag{A-8}$$

where

$$r_{ij}[n]\triangleq\frac{1}{\tilde{N}_o}\int h_i(nT+t)h_j^*(t)\,dt. \tag{A-9}$$

Let

$$r_{ij}(\omega)\triangleq\sum_{k=-\infty}^{\infty}r_{ij}[n]e^{-jk\omega}. \tag{A-10}$$

Using the Poisson sum formula [23], we have

$$r_{ij}(\omega)=\frac{1}{\tilde{N}_oT}\sum_{n=-\infty}^{\infty}H_i\Big(\frac{\omega}{2\pi}-\frac{n}{T}\Big)H_j^*\Big(\frac{\omega}{2\pi}-\frac{n}{T}\Big) \tag{A-11}$$

with

$$H_i(f)=\int_{-\infty}^{\infty}h_i(t)e^{-j2\pi ft}\,dt. \tag{A-12}$$

Denote the Fourier transform of the one-sided sequence $a_0[n](n\le 0)$ as

$$a_0(\omega)\triangleq\sum_{k=-\infty}^{0}a_0[k]e^{-jk\omega} \tag{A-13}$$

and the Fourier transform of the two-sided sequence $a_i[n], i=1,\cdots L,$ as

$$a_i(\omega)=\sum_{k=-\infty}^{\infty}a_i[k]e^{-jk\omega}. \tag{A-14}$$

Then (A-8), $i=1,\cdots,L$ can be written in the frequency domain as

$$a_i(\omega)=-\{(a_0(\omega)-1)r_{i0}(\omega)+\sum_{j=1}^{L}a_j(\omega)r_{ij}(\omega)\} \tag{A-15}$$

or in vector form as

$$\boldsymbol{a}(\omega)=-\{(a_0(\omega)-1)\boldsymbol{r}(\omega)+\boldsymbol{R}(\omega)\boldsymbol{a}(\omega)\}. \tag{A-16}$$

Therefore

$$\boldsymbol{a}(\omega)=(1-a_0(\omega))[\boldsymbol{R}(\omega)+\boldsymbol{I}]^{-1}\boldsymbol{r}(\omega) \tag{A-17}$$

where $\boldsymbol{I}$ is an $L\times L$ identity matrix and

$$\boldsymbol{a}(\omega)=[a_1(\omega),\cdots,a_L(\omega)]^T \tag{A-18}$$

$$\boldsymbol{r}(\omega)=[r_{10}(\omega),\cdots,r_{L0}(\omega)]^T \tag{A-19}$$

and

$$\boldsymbol{R}(\omega)=\begin{pmatrix}r_{11}(\omega)&\cdots&r_{1L}(\omega)\\ \vdots&\vdots&\vdots\\ r_{L1}(\omega)&\cdots&r_{LL}(\omega)\end{pmatrix}. \tag{A-20}$$

Hence, $a_i[n], i=1,\cdots,L$ can be expressed in terms of $a_0[n]$ in the time domain as

$$a_i[n]=b_i[n]-\sum_{k=-\infty}^{0}b_i[n-k]a_0[k] \tag{A-21}$$

where the Fourier transform of $b_i[n]$ is the ith element of the L-element vector function

$$\boldsymbol{b}(\omega)=[\boldsymbol{R}(\omega)+\boldsymbol{I}]^{-1}\boldsymbol{r}(\omega). \tag{A-22}$$

When $i=0$, (A-8) implies that

$$a_0[n]=-\left\{(a_0[0]-1)r_{00}[n]+\sum_{k=-\infty}^{-1}a_0[k]r_{00}[n-k]+\sum_{j=1}^{L}\sum_{k=-\infty}^{\infty}a_i[k]r_{0i}[n-k]\right\} \tag{A-23}$$

for $n\le 0$. By means of (A-21)

$$a_0[n]+\sum_{k=-\infty}^{0}r[n-k]a_0[k]=r[n] \tag{A-24}$$

where

$$r[n] = r_{00}[n] - u[n] \tag{A-25}$$

and

$$u[n] \triangleq \sum_{i=1}^{L} r_{0i}[n] * b_i[n] = \mathcal{F}^{-1}\{\boldsymbol{r}^H(\omega)[\boldsymbol{R}(\omega) + \boldsymbol{I}]^{-1}\boldsymbol{r}(\omega)\}. \tag{A-26}$$

Denote

$$\begin{aligned} r(\omega) &\triangleq \sum_{n=-\infty}^{\infty} r[k]e^{-jn\omega} \\ &= r_{00}(\omega) - \boldsymbol{r}^H(\omega)[\boldsymbol{R}(\omega) + \boldsymbol{I}]^{-1}\boldsymbol{r}(\omega). \end{aligned} \tag{A-27}$$

From [6, Appendix A]

$$\begin{aligned} a_0(\omega) &\triangleq \sum_{n=-\infty}^{0} a_0[n]e^{-jn\omega} \\ &= 1 - \frac{1}{M(-\omega)\gamma_0} \end{aligned} \tag{A-28}$$

where $M(\omega)$ is a stable one-sided Fourier transform

$$M(\omega) = \sum_{n=0}^{\infty} \gamma_n e^{-jn\omega} \tag{A-29}$$

which is uniquely determined by

$$M(\omega)M(-\omega) = r(\omega) + 1. \tag{A-30}$$

The dc component γ_0 in $M(\omega)$ can be found by

$$\gamma_0^2 = \exp\left\{\frac{1}{2\pi}\int_{-\pi}^{\pi} \ln[(r(\omega) + 1]\, d\omega\right\}. \tag{A-31}$$

Substituting (A-28) into (A-17), we have

$$\boldsymbol{a}(\omega) = \frac{1}{M(-\omega)\gamma_0}\,[\boldsymbol{R}(\omega) + \boldsymbol{I}]^{-1}\boldsymbol{r}(\omega). \tag{A-32}$$

Multiplying both sides of (A-5) by $f_o(t)$ and integrating, from (A-4), the MSE of the MMSE-DFE is

$$\begin{aligned} e\{f_o(t)\} &= \sigma^2(1 - a_0[0]) \\ &= \sigma^2 \exp\left\{-\frac{1}{2\pi}\int_{-\pi}^{\pi} \ln\{r(\omega) + 1\}\, d\omega\right\}. \end{aligned} \tag{A-33}$$

REFERENCES

[1] J. H. Winters, "Signal acquisition and tracking with adaptive arrays in the digital mobile radio system IS-136 with flat fading," *IEEE Trans. Veh. Technol.*, vol. 42, pp. 377–384, Nov. 1993.

[2] J. H. Winters, R. D. Gitlin, and J. Salz, "The impact of antenna on the capacity of wireless communication systems," *IEEE Trans. Commun.*, vol. 42, pp. 1740–1751, Feb./Mar./Apr. 1994.

[3] R. L. Cupo, G. D. Golden, C. C. Martin, K. L. Sherman, N. Sollenberger, J. H. Winters, and P. W. Wolniansky, "A four-element adaptive antenna array for IS-136 PCS base station," in *Proc. 47th IEEE Veh. Technol. Conf.*, May 1997, pp. 1577–1581.

[4] P. Monsen, "Feedback equalization for fading dispersive channels," *IEEE Trans. Inform. Theory*, Jan. 1971, pp. 56–64.

[5] ——, "MMSE equalization of interference on fading diversity channels," *IEEE Trans. Commun.*, vol. COM-32, pp. 5–12, Jan. 1984.

[6] J. Salz, "Optimum mean-square decision feedback equalization," *BSTJ*, pp. 1341–1371, Oct. 1973.

[7] P. Balaban and J. Salz, "Optimum diversity combining and equalization in digital data transmission with applications to cellular mobile radio–Part I: Theoretical considerations," *IEEE Trans. Commun.*, vol. 40, pp. 885–894, May 1992.

[8] ——, "Optimum diversity combining and equalization in digital data transmission with applications to cellular mobile radio–Part II: Numerical results," *IEEE Trans. Commun.*, vol. 40, pp. 895–907, May 1992.

[9] Y. Li and Z. Ding, "A simplified approach to optimum diversity combining and equalization in digital data transmission," *IEEE Trans. Commun.*, vol. 43, pp. 2285–2288, Aug. 1995.

[10] M. Clark, L. J. Greenstein, W. K. Kennedy, and M. Shafi, "Optimum linear diversity receivers for mobile communications," *IEEE Trans. Veh. Technol..*, vol. 43, pp. 47–56, Feb. 1994.

[11] B. R. Petersen and D. D. Falconer, "Minimum mean square equalization in cyclostationary and stationary interference-analysis and subscriber line calculations," *IEEE J. Select. Areas Commun.*, vol. 9, pp. 931–940, Aug. 1991.

[12] ——, "Suppression of adjacent-channel cochannel, and intersymbol interference by equalizers and linear combiners," *IEEE Trans. Commun.*, vol. 42, pp. 3109–3118, Dec. 1994.

[13] Y. Sato, "A method of self-recovering equalization for multi-level amplitude modulation," *IEEE Trans. Commun.*, vol. COM-23, pp. 679–682, June 1975.

[14] D. N. Godard, "Self-recovering equalization and carrier tracking in two-dimensional data communication systems," *IEEE Trans. Commun.*, vol. COM-28, pp. 1867–1875, 1980.

[15] J. R. Treichler and B. G. Agee, "A new approach to multipath correction of constant modulus signals," *IEEE Trans. Acoust., Speech, Signal Processing*, vol. ASSP-31, pp. 459–471, Apr. 1985.

[16] G. J. Foschini, "Equalization without altering or detect data," *AT&T Tech. J.*, pp. 1885–1911, Oct. 1985.

[17] Y. Li and Z. Ding, "Global convergence of fractionally spaced Godard equalizer," *IEEE Trans. Signal Processing*, vol. 44, pp. 818–826, Apr. 1996.

[18] G. E. Bottomley and K. Jamal, "Adaptive arrays and MLSE equalization," in *Proc. 45th IEEE Veh. Technol. Conf.*, July 1995, pp. 50–54.

[19] K. J. Molnar and G. E. Bottomley, "D-AMPS performance in PCS bands with array processing," in *Proc. 46th IEEE Veh. Technol. Conf.*, Apr. 1996, pp. 1–5.

[20] W. C. Jakes, Jr., Ed. *Microwave Mobile Communications*. New York: IEEE Press, 1974.

[21] H. L. Van Trees, *Detection, Estimation, and Modulation Theory, Part III*. New York: Wiley, 1968.

[22] J. Fuhl and E. Bonek, "Space–time decomposition: Exploiting the full information of a training sequence for an adaptive array," *Electron. Lett.*, vol. 32, pp. 1938–1940, Oct. 1996.

[23] J. Proakis, *Digital Communications*, 2nd ed. New York: McGraw-Hill, 1989.

[24] L. J. Greenstein, V. Erceg, Y.-S. Yeh, and M. V. Clark, "A new path-gain/delay-spread propagation model for digital cellular channels," *IEEE Trans. Veh. Technol.*, vol. 46, pp. 477–485, May 1997.

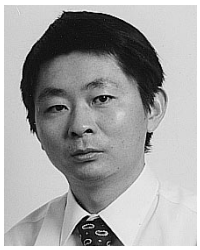

Ye (Geoffrey) Li (S'92–M'95–SM'97) received the B.Eng. and M.Eng. degrees in 1983 and 1986, respectively, from the Nanjing Institute of Technology, Nanjing, China, and the Ph.D. degree in 1994 from Auburn University, Auburn, AL.

From March 1986 to May 1991, he was a Teaching Assistant and then a Lecturer with the National Mobile Communication Laboratory, Southeast University, China. From September 1991 to September 1994, he was a Research and Teaching Assistant with the Department of Electrical Engineering, Auburn University. From September 1994 to May 1996, he was a Post-Doctoral Research Associate with the Department of Electrical Engineering and Institute for Systems Research, University of Maryland at College Park. Since May 1996, he has been with the Wireless Systems Research Department, AT&T Labs-Research, Red Bank, NJ. His general research interests include statistical signal processing and wireless mobile systems with emphasis on signal processing in communications.

Jack H. Winters (S'77–M'81–SM'88–F'96) received the B.S.E.E. degree from the University of Cincinnati, Cincinnati, OH, in 1977 and the M.S. and Ph.D. degrees in electrical engineering from Ohio State University, Columbus, in 1978 and 1981, respectively.

Since 1981, he has been with AT&T Bell Laboratories and now AT&T Labs-Research, Red Bank, NJ, where he is in the Wireless Systems Research Department. He has studied signal processing techniques for increasing the capacity and reducing signal distortion in fiber optic, mobile radio, and indoor radio systems and is currently studying adaptive arrays and equalization for indoor and mobile radio.

Nelson R. Sollenberger (S'78–M'81–SM'90–F'96) received the Bachelor's degree from Messiah College, Grantham, PA, in 1979 and the Master's degree in 1981 from Cornell University, Ithaca, NY, both in electrical engineering.

From 1979 to 1986, he was a member of the cellular radio development organization at Bell Laboratories. At Bell Laboratories, he investigated spectrally efficient analog and digital technologies for second-generation cellular radio systems. In 1987, he joined the Radio Research Department at Bellcore and was the Head of that department from 1993 to 1995. At Bellcore, he investigated concepts for PACS, the personal access communications system. He heads the Wireless Systems Research Department at AT&T, Red Bank, NJ. His department performs research on next-generation wireless systems concepts and technologies including high-speed transmission methods, smart antennas and adaptive signal processing, system architectures and radio link techniques to support wireless multimedia, and advanced voice services.